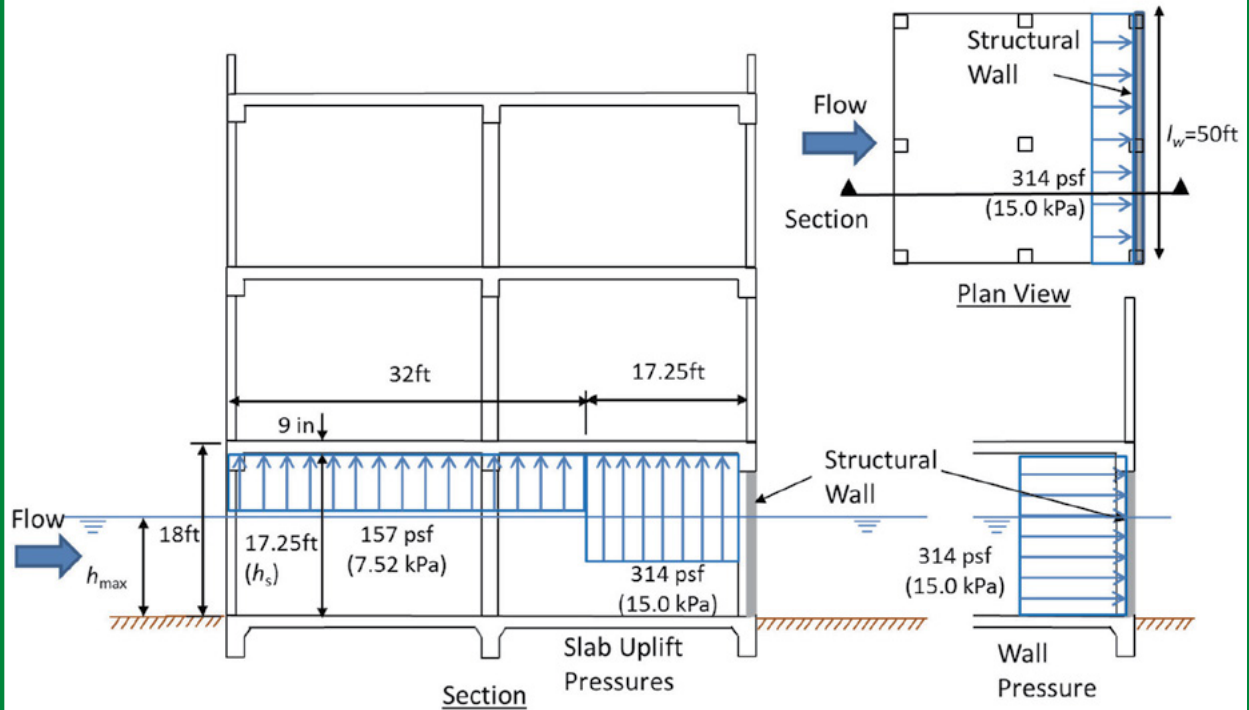


Example G10-18. Wall-Slab Recess Pressure.

The same building used in **Example G10-17** is exposed to bore conditions with a structural wall blocking the flow at the back of the ground-floor level as shown in the figure. Based on ASCE 7-16, Section 6.6.4, bore conditions are anticipated at the site. The energy grade line analysis gives the maximum flow depth at the site as $h_{\max} = 15$ ft, and the maximum velocity as $u_{\max} = 20$ ft/s. Load Case 2 flow depth is $h = 2/3 h_{\max} = 10$ ft.



The flowchart in **Figure G10-21** provides the following guidance:

1. Do bore conditions exist? Yes
2. Is $F_r > 1.0$? Yes

The Froude number at the site is $F_r = \frac{u}{\sqrt{gh}} = \frac{20}{\sqrt{32.2 \times 10}} = 1.11 > 1.0$.

3. Is the slab height greater than $3.5h$? No

$$h_s = 17.25 \text{ ft} \not> 3.5 \times h = 3.5 \times 10 = 35 \text{ ft}$$

4. Is h greater than two-thirds slab height? No

$$h_{\max} = 10 \text{ ft} \not> \frac{2}{3} \times h_s = \frac{2}{3} \times 17.25 = 11.5 \text{ ft}$$

Therefore, the wall and slab within $h_s = 17.25$ ft of the wall must be designed for the uplift pressure given by ASCE 7-16, Equation (6.10-10), and the rest of the slab must be designed for half of this pressure

$$P_u = I_{TSU} \left(590 - 160 \frac{h_s}{h} \right) = 1.0 \left(590 - 160 \frac{17.25}{10} \right) = 314 \text{ psf}$$

This uplift pressure reduces to $P_u = 0.5 \times 314 = 157$ psf for the slab further than 17.25 ft from the back wall. Because there are no side walls preventing the flow from passing around the ends of the back wall, this pressure of 157 psf can be reduced to 30 psf at a distance $h_s + l_w = 17.25 + 50 = 67.25$ ft away from the wall. This does not occur in the given building because it exceeds the building length.

$P_{ur} = C_{cx} P_u$, where P_u is given by Equation (6.10-10) for the solid wall condition. **Example G10-19** shows the application of this provision to determine the hydrodynamic pressures in a building with a perforated structural wall restricting flow through the ground-floor level.

10.3.3.4 Reduction of Load for Slab Openings

During the Tohoku tsunami, concrete access panels and steel grating spanning between the pile-supported wharves and the soil-supported dock allowed for relief of some of the pressure developed below the wharf (**Figure G10-20**). Experiments in a wave flume at the University

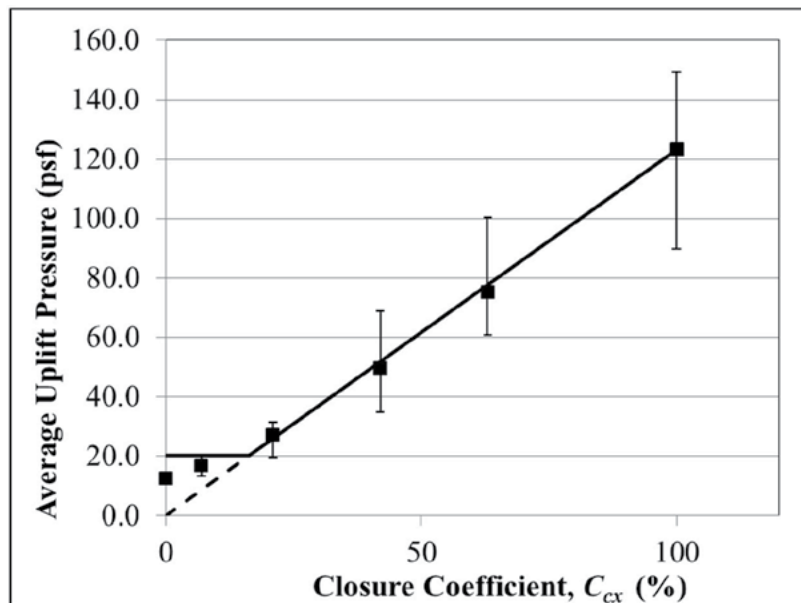
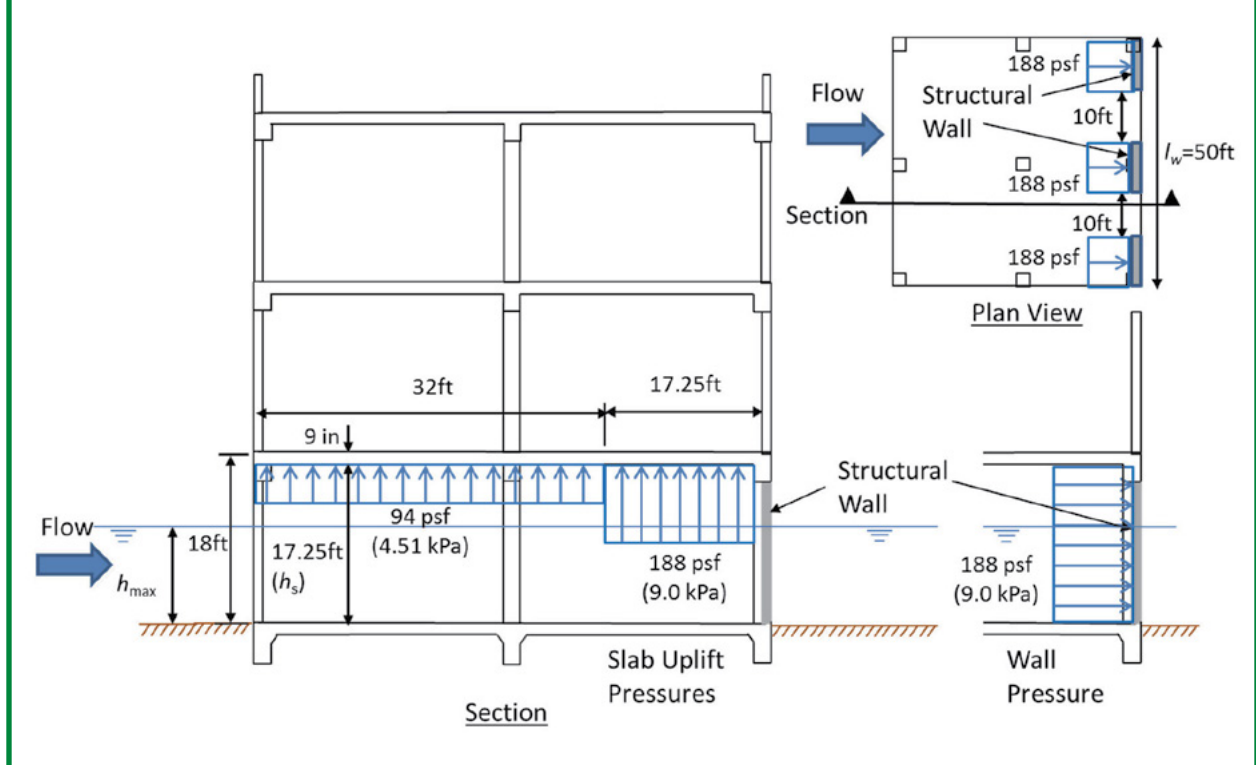


Figure G10-24. Change in slab uplift pressure with varying closure coefficient for the back wall in a slab-wall recess subjected to bore loading.

Example G10-19. Wall-Slab Recess with Perforated Wall.

The same building used in **Example G10-17** is exposed to the same bore conditions, but with a series of three structural piers, each 10 ft wide, blocking the flow at the back of the ground floor level as shown in the figure. The closure coefficient is therefore given by $C_{cx} = (3 \times 10)/50 = 0.6$. Therefore, the pressures will be 60% of those found for the solid wall in **Example G10-17**. For the wall piers and the slab within $h_s = 17.25$ ft of the wall, $P_{ur} = 0.6 \times 314 = 188$ psf. For the rest of the slab, $P_{ur} = 0.6 \times 157 = 94$ psf as shown in the figure.



of Hawai'i at Manoa using a bore generated by dam break confirmed these results (Takakura and Robertson 2010). The test setup for these experiments is shown in **Figure G10-25**. The clear slab height, h_s , and gap width, w_g , were varied to study the effect on the average slab uplift pressure. **Figure G10-26** shows how the uplift on the slab reduces with the increased gap width. Two slab heights were considered, and a number of different bore scenarios were generated by the dam break. The curves are plotted through the mean test results, with the range of results shown by the error bars. When the gap width equals half the slab height, the uplift is reduced by more than 50%. The effect is less dramatic as the gap increases further. ASCE 7-16, Equations (6.10-13) and (6.10-14) are based on these data and shown by the dashed lines in **Figure G10-26**. **Example G10-20** shows how these pressures are determined for a building with a structural wall preventing flow through the ground-floor level, but a break-away panel provided in the second-level floor slab.

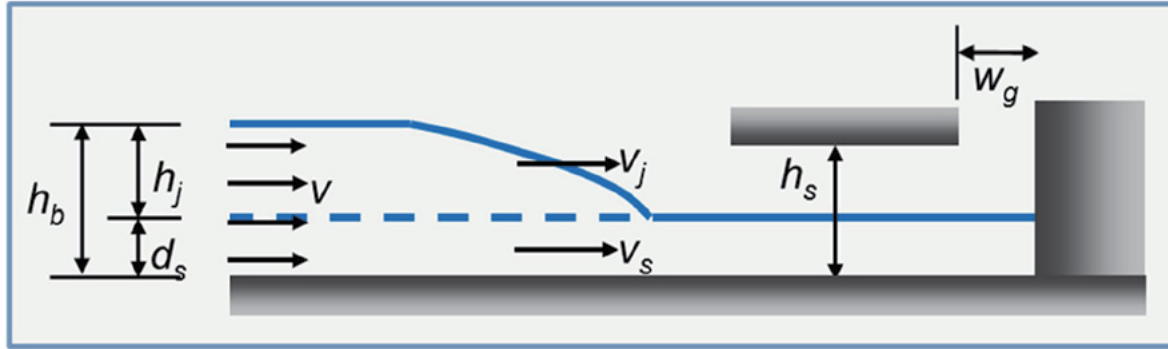


Figure G10-25. Test setup to study the effect of a slab opening on the uplift pressure when a bore enters a slab-wall recess.

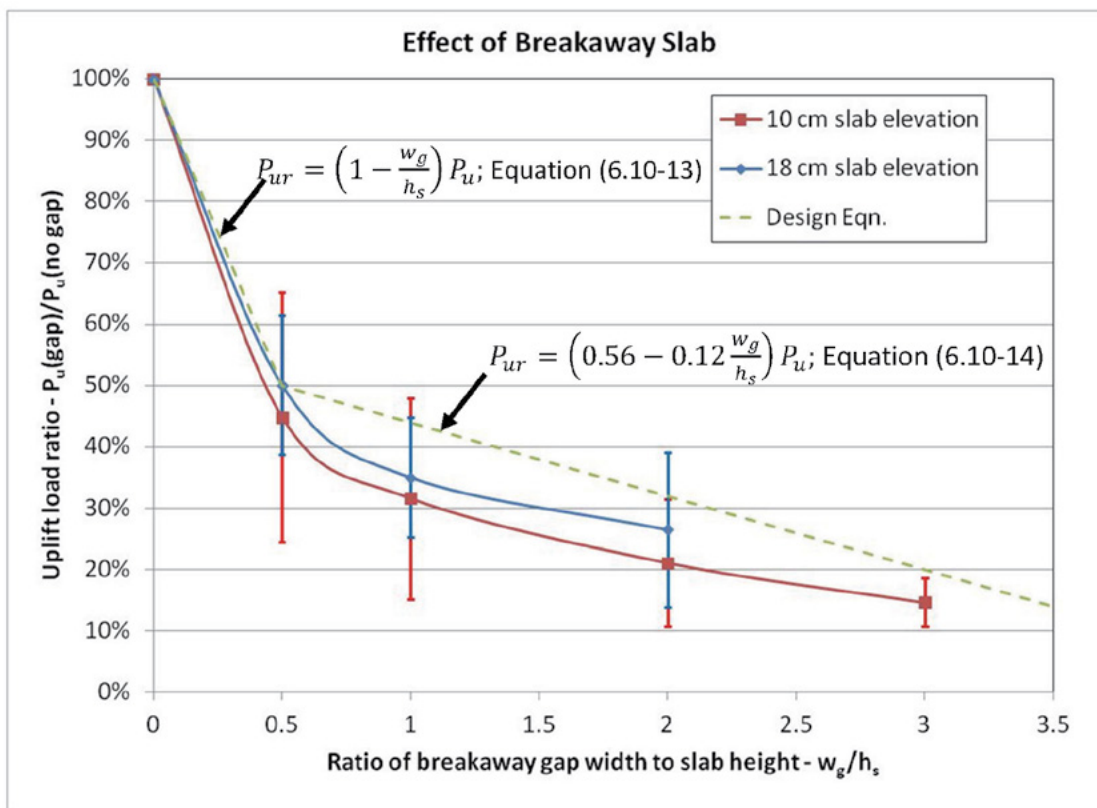


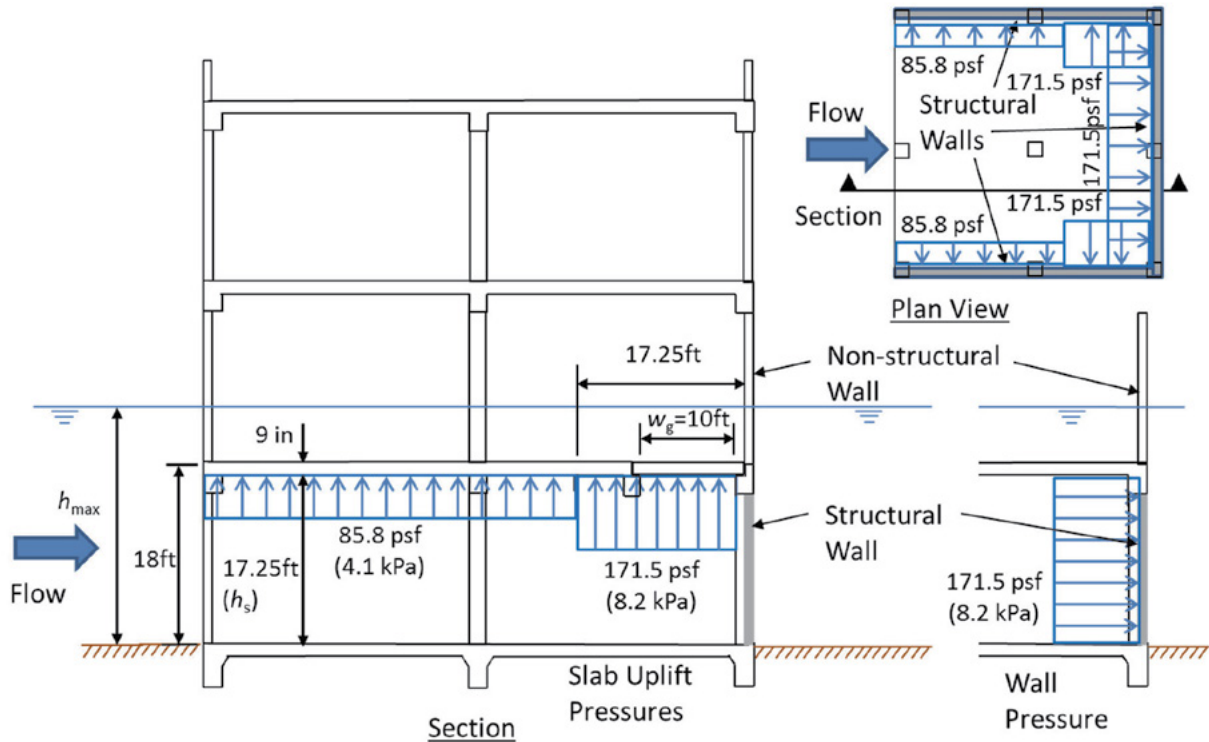
Figure G10-26. Effect of slab opening width on average uplift pressure.

10.3.3.5 Reduction in Load for Tsunami Breakaway Wall

If the wall blocking flow through the building is designed as a tsunami breakaway wall, then the maximum pressure that needs to be considered on the slab adjacent to the wall is equal to the pressure required to reach the nominal shear force necessary to fail the breakaway wall. This failure is usually governed by separation of the wall from the slab at top or bottom of the wall. Estimating this nominal shear force should take into account the likely overstrength of the connection fasteners and hardware involved in making the connection between the breakaway wall and slab.

Example G10-20. Wall-Slab Recess with Breakaway Slab.

The same building used in **Example G10-17** is exposed to the same bore conditions. The slab is constructed with a loose breakaway panel adjacent to the back wall as shown in the figure. The clear opening for the gap is 10 ft wide, and the gap runs the full width of the building.



Because $w_g = 10$ ft is greater than $0.5h_s = 0.5 \times 17.25 = 8.625$ ft, ASCE 7-16, Equation (6.10-14) is used to determine the effect of the breakaway slab as

$$C_{bs} = 0.56 - 0.12 \frac{w_g}{h_s} = 0.56 - 0.12 \frac{10}{17.25} = 0.49$$

Therefore, the uplift pressure on the slab soffit given by ASCE 7-16, Equation (6.10-12) is

$$P_{ur} = C_{bs} P_u = 0.49 \times 350 = 171.5 \text{ psf}$$

This pressure is applied to the wall and the slab within $h_s = 17.25$ ft of the wall (including the breakaway panel). For the rest of the slab, $P_{ur} = 0.5 \times 171.5 = 85.8$ psf as shown in the figure.

To verify that this pressure is sufficient to lift the breakaway panel, we must check that it exceeds the dead weight of the panel

$$w_D = \gamma_{conc} V = 150 \times \frac{9}{12} \times 1 \times 1 = 112.5 \text{ psf}$$

Because 171.5 psf is greater than 112.5 psf, the slab will lift and release the pressure below the slab. If the slab weight was greater than 171.5 psf, then the wall-slab recess pressure would be increased to match the slab weight. Alternatively, the slab weight could be reduced by using lightweight concrete or a thinner slab for the breakaway panel.

Care should be taken to design the columns at the second level to resist impact from these breakaway slabs following the procedure in ASCE 7-16, Section 6.11.4, “Submerged Tumbling Boulder and Concrete Debris,” even if these columns would not normally be exposed to debris impact.

Debris Impact Loads

During coastal inundation, large amounts of floating and rolling debris are transported by the tsunami. During the 2011 Tohoku tsunami, the debris consisted of everything from small plastic items to very large ships. This section addresses the impact loads that need to be considered in structural design owing to the potential for debris striking a structural member. Debris impact strikes need not be considered if the flow depth is less than 3 ft since only smaller items will float under this condition.

ASCE 7-16 considers five specific debris items, which are considered representative of the more damaging types of debris found in a typical tsunami flow. These debris types are

1. Wood poles and logs, which are generated when the flow causes failure of trees, power poles, and large timber structures.
2. Floating vehicles in the form of cars and trucks that are buoyant until water is able to seep into the enclosed passenger compartment.
3. Submerged and tumbling boulder and concrete debris represents large dense items that do not float but are rolled along the ground by the tsunami. Flow conditions have to be adequate to initiate movement of these objects, but once they are moving, they can induce significant impact damage just above grade level. These impacts need not be considered if the flow depth at the site is less than 6 ft.
4. Shipping containers are universally used to transport goods through ports worldwide. Large quantities of these containers both empty and with contents are stored at most cargo ports, making them susceptible to flotation during a tsunami. Limits on the maximum weight of a loaded shipping container are set so that they can still be handled by the port equipment. This total weight is about one-third of the buoyant force for the closed container, so all containers will float if they are closed and subjected to more than about 3 ft of water (**Review G11-1**).
5. Large ships and barges represent a major impact threat to buildings and other structures adjacent to ports. However, they require significant draft before they will float. ASCE 7-16 only requires that these impacts be considered in the vicinity of ports and harbors if the flow depth at the site exceeds 12 ft.

Review G11-1. Shipping Container Buoyancy.

A standard 20 ft shipping container has a self-weight of 5,400 lb. Maximum total weight limit for a standard 20 ft container is 53,000 lb. The container dimensions are 20 ft long by 8 ft wide by 8.5 ft high (or 9.5 ft for high cube).

For an empty 20 ft container to float, $F_{\text{Buoyancy}} \geq W_{\text{Container}}$, or, $\gamma_s V = 70.4(20 \times 8 \times d) \geq 5,400 \therefore d \geq 0.48$ ft will cause the empty container to float.

For a sealed fully loaded container to float, $\gamma_s V = 70.4(20 \times 8 \times d) \geq 53,000 \therefore d \geq 4.7$ ft will cause the container to float.

“Heavy tested” 20 ft containers have a maximum weight of 67,200 lb and therefore require 6.0 ft of water to float.

Although the self-weight (8,800 lb) and maximum weight (67,200 lb) of a 40 ft container are larger than the standard 20 ft container, so is the displaced volume. The result is that an empty 40 ft container will float in 0.39 ft of water, whereas a fully loaded 40 ft container will float in 3.0 ft of water.

ASCE 7-16 only requires consideration of shipping container debris impact when the inundation depth exceeds 3 ft (Section 6.11).

Figure G11-1 provides a flowchart that identifies the types of debris that must be considered at a particular site. Debris impacts can occur during both incoming and outgoing flow, but their effects need only be considered when designing perimeter gravity load-carrying structural components. Damage to a gravity load-carrying structural component such as a column can lead to progressive collapse of a portion or all of the building, potentially resulting in loss of life for those who might have sought refuge in the building. Interior structural members are considered to be protected from debris by the perimeter members, or at least the debris velocity is assumed to have decreased significantly if the debris is able to enter the interior of a structure.

Floating debris is assumed to travel at the flow velocity, as confirmed by laboratory experiments on a one-fifth scale shipping container in the Large Wave Flume at Oregon State University (Riggs et al. 2014). Debris impact is considered to be a single concentrated force acting anywhere within the flow depth since the debris may not always travel at the water surface. The impact loads must be applied to the structural member at locations that cause maximum bending moment and maximum shear force in the member.

Debris impact loads need not be considered to act simultaneously on multiple members.

The impact duration is extremely short, and the probability of multiple simultaneous strikes is therefore very low.

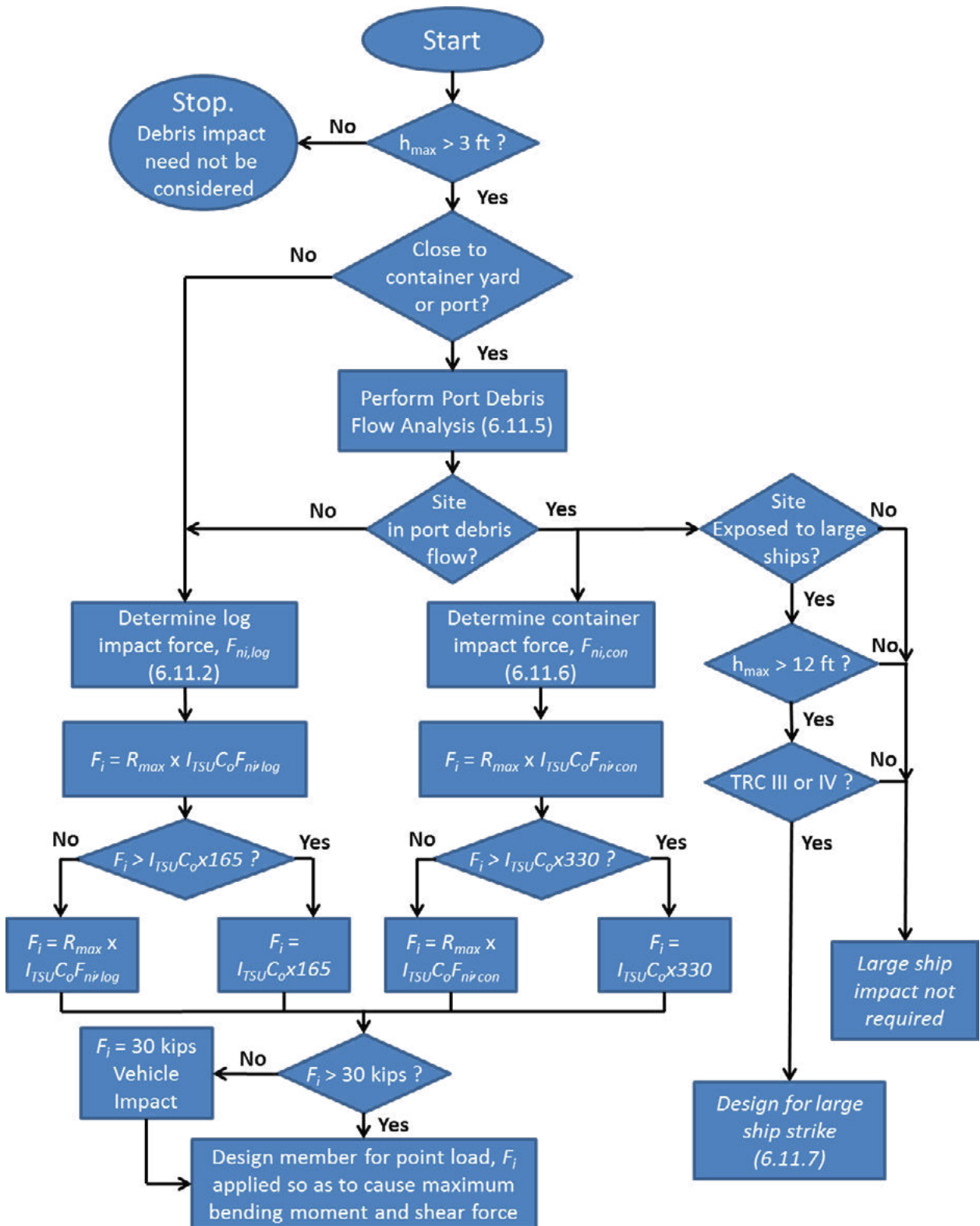


Figure G11-1. Flowchart for debris impact.

Debris impact loads need not be considered to act simultaneously on multiple members since the impact duration is extremely short and the probability of multiple simultaneous strikes is very low. In addition, other tsunami-related loads, such as hydrodynamic and hydrostatic loads, need not be combined with the debris impact loads. Because of conservatism in the debris impact loading and the low probability that a direct strike from a shipping container, log, or other large debris object occurs at the peak hydrodynamic or hydrostatic load, it is not required that these loads be considered simultaneously.

Debris strikes are highly impulsive in nature and will result in dynamic excitation of the impacted structural element. When debris strikes a structural element, the impact duration can be extremely short. If this duration is similar to the natural period of vibration of the structural element, the dynamic effects can lead to an increased force in the element. This dynamic amplification can be approximated by using the R_{\max} factor from ASCE 7-16, Table 6.11-1. However, it is more accurate, and generally less conservative, to consider dynamic analysis of the structural element response to a rectangular pulse as described in ASCE 7-16, Section 6.11.8. This approach can be used for both elastic and inelastic structural response and will generally produce the most accurate structural design. For impacts in which the structural element exceeds its elastic limit, work-energy methods may also be used (ASCE 7-16, Section 6.11.8).

11.1 Alternative Simplified Debris Impact Static Load

As the tsunami flow velocity increases, so do the potential impact forces from debris floating in that flow. However, if the impact force exceeds the axial capacity of the debris material, then the force will be limited to the material axial capacity. For a log impact, unless the end of the log is perfectly flat and strikes the structural element perfectly perpendicular, it is appropriate to assume that only a portion of the log end area will be crushed during the impact. ASCE 7-16 assumes a contact area equal to 20% of the cross-sectional area of a 1 ft diameter log, or approximately 22 in.² Assuming a timber crushing strength of 5,000 psi, representing approximately the mean plus one standard deviation for Southern pine or Douglas fir according to ASTM D2555 (2017), the resulting crushing force is 110 kips. Including a dynamic response factor of 1.5 results in the basic direct strike force of $F_i = 165C_oI_{TSU}$ kips. This represents 50% of the force given in ASCE 7-16, Section 6.11.1, which applies to sites that are not in an impact zone for shipping containers, ships, and barges.

Similarly, tests at Lehigh University using a full-scale 20 ft shipping container showed that the maximum impact force was limited to the combined yielding and buckling strength of the axial member running along the bottom corners of the container (Piran Aghl et al. 2014). These are the strongest structural elements making up the container shell, and their axial stiffness results in the largest impact loads if the container is oriented with its long axis parallel to the flow. For this condition, the maximum impact force was 311 kips when both